Graphene Oxide Assisted Hydrothermal Carbonization of Carbon Hydrates

Deepti Krishnan,[†] Kalyan Raidongia,[†] Jiaojing Shao,[†,‡] and Jiaxing Huang[†,*]

[†]Department of Materials Science and Engineering, Northwestern University, Evanston, Illinois 60208, United States, and [‡]Key Laboratory for Green Chemical Technology of Ministry of Education, School of Chemical Engineering and Technology, Tianjin University, Tianjin, China

ABSTRACT Hydrothermal carbonization (HTC) of biomass such as glucose and cellulose typically produces micrometer-sized carbon spheres that are insulating. Adding a very small amount of Graphene oxide (GO) to glucose (*e.g.*, 1:800 weight ratio) can significantly alter the morphology of its HTC product, resulting in more conductive carbon materials with higher degree of carbonization. At low mass loading level of GO, HTC treatment results in dispersed carbon platelets of tens of nanometers in thickness, while at high mass loading levels, free-standing carbon monoliths are obtained. Control experiments with other carbon materials such as graphite, carbon nanotubes, carbon black, and reduced GO show that only GO has significant effect in promoting HTC conversion, likely due to its good water processability, amphiphilicity, and two-dimensional structure that may help to template the initially carbonized materials. GO offers an additional advantage in that its graphene product can act as an *in situ* heating element to enable further carbonization of the HTC products very rapidly upon microwave irradiation. Similar effect of GO is also observed for the HTC treatment of cellulose.

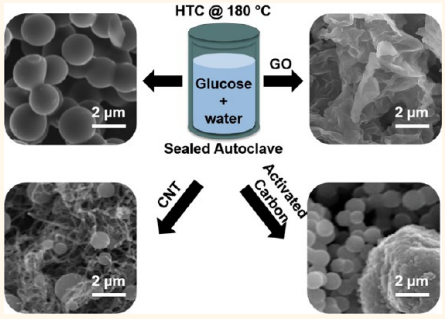

KEYWORDS: biomass · carbon hydrates · carbonization · graphene oxide · hydrothermal · microwave

Increasing energy demand due to rapid growth in population and industrialization along with environmental crisis has led to the search for cheap, environmentally friendly, and nontoxic materials for generation and storage of energy. Biomass is abundant and has been shown to be an efficient renewable resource for synthesizing functional carbonaceous materials. Hydrothermal carbonization (HTC) is one of the most promising techniques to convert biomass.[1−10] HTC was first introduced by Bergius and Specht in 1913 who described the hydrothermal transformation of cellulose into coal-like materials.[11] It was followed by the systematic investigations performed by Berl and Schmidt in 1932, where they alternated the source of biomass and treated the various samples, at temperatures from 150 to 350 °C, in the presence of water.[12] Their sequence of papers published in 1932 gave knowledge of those days about the emergence of coal.[13] Starting from the new century, significant new interest in HTC has emerged followed by the synthesis of carbon spheres.[14,15] Typically, the reaction involves hydrothermal heating of biomass at mild temperatures (∼200 °C) under self-generated pressure in a closed container. Consequently, a variety of functional carbonaceous materials have been synthesized from biomass *via* the HTC process for potential applications in energy storage,[2,3,15,16] water purification,[1] hydrogen storage,[16] and catalysis.[17]

Since cellulose is one of the main components in lignocellulosic biomass and glucose is the major structural unit and acid digestion product of biomass, they have often been used as a model system in HTC studies. HTC treatment of glucose or cellulose typically produces well-dispersed, micrometer-sized carbon spheres.[14,15] However, these spheres are insulating and need to be further carbonized by annealing to become conductive. Graphene oxide (GO) is the chemical exfoliation product of graphite powders, which has been extensively pursued as a precursor for bulk production of chemically modified graphene (*i.e.*, reduced GO, r-GO) in recent years.[18−24] Like graphene, GO is also a two-dimensional (2D) single atomic sheet but has

* Address correspondence to jiaxing-huang@northwestern.edu.

Received for review September 13, 2013 and accepted December 3, 2013.

Published online December 03, 2013
10.1021/nn404805p

many interesting properties of its own.[25−29] GO sheets have rich oxygenated functional groups decorating the segregated nanographitic domains on their basal plane[30] and are easily dispersed in water and many polar solvents. In earlier works, we have found that GO sheets are amphiphilic and can help to disperse insoluble materials such as graphite and carbon nanotubes in water.[31,32] When interacting with other materials containing π-conjugated units, GO sheets are also capable of templating their assembly and even altering their molecular configurations.[33−36] On the basis of the above knowledge, we hypothesize that GO could act as a water-dispersible yet still graphitic structural template to promote the carbonization of glucose and/or cellulose under hydrothermal conditions. Here we report that graphene oxide (GO) can assist the HTC process of glucose and cellulose, leading to products with higher degree of carbonization and conductivity under the same reaction conditions at a catalytic amount (GO/glucose weight ratio up to 1:800). Moreover, the embedded r-GO sheets can serve as an *in situ* heating element upon microwave irradiation, which allows rapid annealing of the HTC carbon to achieve even higher degree of carbonization and crystallinity.

RESULTS AND DISCUSSION

Glucose is the basic sugar building block of biomass,[37] which has been extensively studied for synthesizing functional carbon sphere materials by HTC. Under hydrothermal conditions at relatively low temperatures (<200 °C), glucose molecules underwent a series of dehydration and cross-linking reactions and eventually turned into carbonized spherical colloidal particles dispersed in water,[14,37] as shown in the scanning electron microscope (SEM) image in Figure 1a. The final yield of carbon spheres was about 10% by mass. Adding a small amount of GO to the reaction (final GO concentration 0.02 mg/mL, GO/glucose weight ratio of 1:300) did not affect the conversion yield but completely altered the morphology of the HTC product. As shown in the SEM image in Figure 1b, no carbon spheres are obtained and the resulting materials appear to be platelets. Atomic force microscopy (AFM) studies (Figure 1c,d) show that the platelets obtained from HTC treatment of GO/glucose indeed resemble the appearance of GO sheets in terms of size and shape. The apparent thickness of GO sheets is around 1 nm (Figure 1c). However, the HTC platelets have an apparent thickness of around 40 nm (Figure 1d). Since no carbon spheres were observed, this implies that GO sheets can act as nucleation and growth sites for seeding the carbonization product of glucose.

The degree of carbonization or defunctionalization of the HTC products was examined by Fourier transform infrared (FTIR) spectroscopy. Figure 2a compares

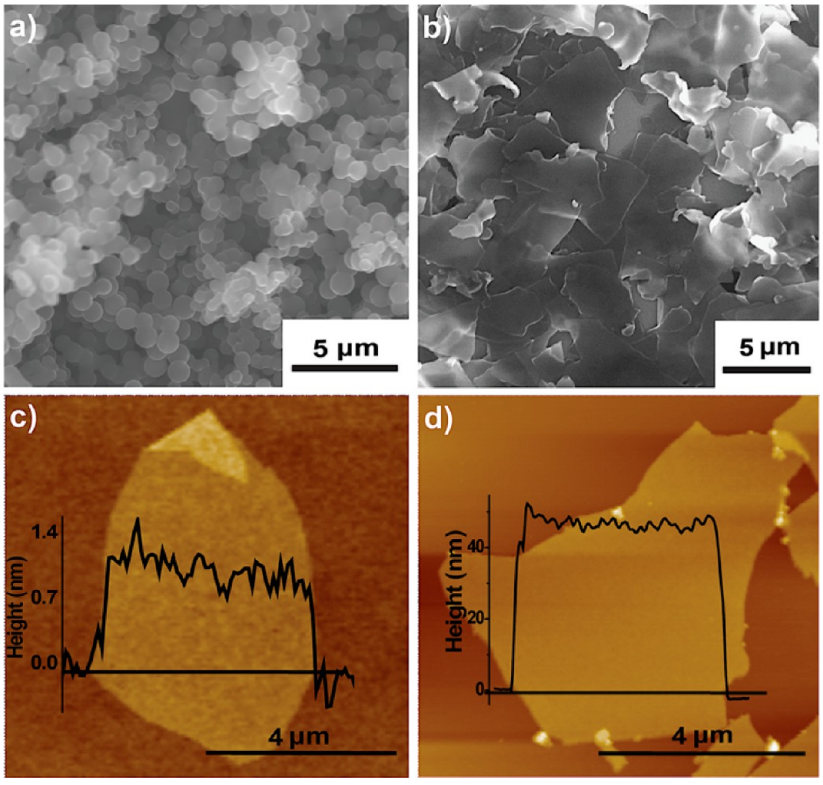

Figure 1. (a) SEM image of the carbon spheres obtained after HTC of glucose at 180 °C for 16 h. (b) SEM image of the platelets obtained after HTC of GO and glucose at a weight ratio of 1:300 at 180 °C for 16 h. The overall GO concentration was 0.02 mg/mL. (c) AFM image of a GO sheet with line scan showing thickness of around 1 nm. (d) AFM image of the platelet obtained after HTC of GO and glucose. The line scan shows the thickness is increased to around 40 nm.

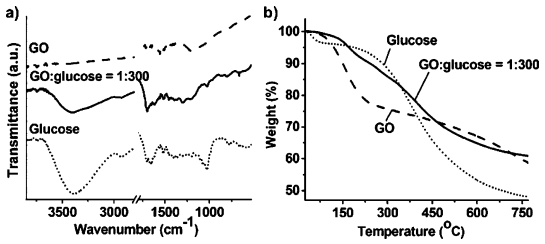

Figure 2. (a) FTIR spectra and (b) TGA curves of the platelets obtained after HTC of a GO and glucose mixture (1:300), compared with those of pure GO and glucose treated under similar conditions (180 °C for 16 h), respectively. The concentration of GO was maintained at 0.02 mg/mL. TGA was carried out in N_2 atmosphere at a heating rate of 10 °C/min. The steady weight loss in the temperature regime of 200 to 600 °C corresponds to thermal decomposition of functional groups.

the IR spectra of HTC products of GO, glucose, and their mixture. The spectrum of the carbon spheres obtained from glucose (Figure 2a, dotted line) has two bands at around 1700 and 1650 cm^{-1}, which are attributed to −C═O and −C═C groups, respectively. This confirms dehydration and aromatization of glucose during the HTC treatment. The bands centered at around 3400 and 1030 cm^{-1} represent the stretching and bending modes of the residual −OH group, respectively. IR spectrum of the platelets (Figure 2a, solid line) shown in Figure 1b looks very similar to that of the carbon spheres. However, the relative intensity of the peaks at around 3400 and 1030 cm^{-1} decreased significantly. Although hydrothermal treatment of GO does produce even more graphitic r-GO (Figure 2a, dashed line),[38] since only 0.3 wt % of GO was added to glucose, the decrease in the intensity of −OH bands should be attributed to enhanced degree of carbonization of glucose.

The thermogravimetric analysis (TGA) curves of the above-mentioned HTC products are shown in Figure 2b. There is a significant difference in their thermal degradation characteristics. The thermal degradation of glucose-derived carbon spheres undergoes two major weight loss stages. A first minor weight loss of around 5 wt % occurred at around 100 °C, which corresponds to the removal of moisture and volatile matter. Another major weight loss of nearly an additional 50 wt % occurred between 200 and 750 °C, which corresponds to the cracking of organic compounds. The platelets obtained from GO/glucose exhibited much better thermal stability, showing only around 40% total weight loss when heated to 750 °C, which is comparable to the final weight loss of GO in the same temperature range. Under our HTC conditions, the yield of glucose carbonization is around 10 wt %. When GO is converted to r-GO after HTC treatment, the weight loss should be around 50%.[28] Assuming all GO sheets have turned into r-GO embedded in the platelets, the r-GO content should be around 1.7 wt %. Therefore, the over 10% difference in weight loss between the HTC products with and without GO cannot be attributed to a simple mixture of r-GO and HTC carbon. Figure 2b clearly shows that adding a small amount of GO (and its r-GO product) greatly improves the thermal stability of HTC product and even makes it comparable to that of r-GO. The FTIR and TGA results both indicate that higher degree of carbonization and graphitization of glucose has been achieved by adding GO to the HTC reaction.

As reported earlier by Xu *et al.*,[39] we found that HTC treatment of GO at higher concentration (*e.g.*, 1 mg/mL) creates a three-dimensional (3D) monolith of r-GO foam. Adding 1 mg/mL of GO into glucose solution also resulted in monolith-like HTC products for a wide range of GO/glucose ratios up to 1:800. It is quite remarkable that such a small ratio of GO can influence the reaction product of a large quantity of glucose. The sizes of the monoliths increased with increasing amount of glucose in the reaction mixture. Figure 3a shows a photo of the freeze-dried monoliths obtained by the HTC of 15 mL aqueous solution containing 15 mg of GO with glucose amount varied from 0 to 6000 mg. The weight of the monoliths increased linearly with increasing amount of glucose in the starting reaction mixture, as shown in Figure 3b. The linear increase in the monolith weight indicates that glucose is being used efficiently in the monolith formation even at very high concentrations. The effect of GO in the kinetics of HTC reaction is shown in Figure 3c using the HTC reaction of GO/glucose ratio of 1:400 as an example. To follow the reaction progress, two sets of parallel HTC reactions of glucose with and without the addition of GO were carried out with reaction time increased from 1, 2, 3, 4, 5, 6, 9, 12, 15, 16, and 21 h. The solid products were collected by first quenching the autoclaves in cold water, followed by filtration. Figure 3c shows that hydrothermal treatment of glucose did not generate solid product within the first 3 h. The amount of solid product increased nearly linearly afterward, and the reaction reached near completion at 15 h. However, with GO sheets added, the reaction started after just 1 h and proceeded much more rapidly. Nearly 60% of the final product was already produced within the first 3 h. The reaction rate slowed down afterward, likely due to depletion of carbon precursors. Figure 3c clearly shows that GO sheets can significantly accelerate HTC reactions of glucose.

The SEM images in Figure 4a−f reveal the evolution of microstructures of the monolithic carbon products obtained with increasing amount of glucose in the precursor. As reported before,[39] the monolith obtained from neat GO is made of interconnected graphene sheets forming a porous structure (Figure 4a). With increasing GO/glucose ratios up to 1:300, the resulting monoliths have similar open structure and are also made of sheet-like building blocks but with increasing thicknesses, suggesting that glucose carbonization

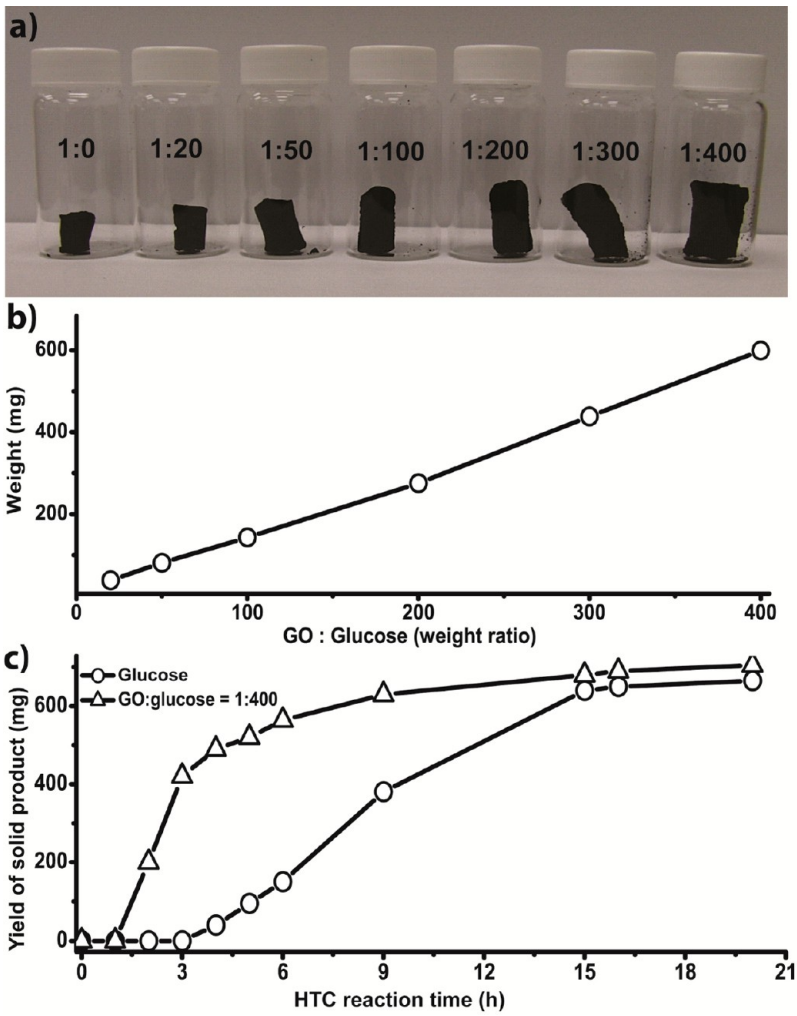

Figure 3. (a) At a concentration of 1 mg/mL, hydrothermal treatment of GO solution leads to a r-GO monolith (first vial on the left). Hydrothermal treatment of GO (1 mg/mL) and glucose mixture can also create monoliths with GO/glucose weight ratios up to 1:400 as shown in the photo. (b) Weight of the monoliths increased linearly with increasing glucose content. (c) Yields of solid product over reaction time showing that the presence of GO accelerates the rate of carbonization (as indicated by the product yield), especially during the initial stage of the reaction.

product is uniformly coating the r-GO sheets as those observed in Figure 1. With GO/glucose ratio of 1:400, the resulting monolith is no longer porous and no platelet structure can be observed as they may have been embedded in glucose-derived carbon (Figure 4d). With further increase of glucose content to 1:800, the surface of the monolith starts to grow hemispherical buds, resembling the shape of the carbon spheres obtained without GO (Figure 4e). With GO/glucose ratio of 1:1000, the main HTC product is observed to be carbon spheres again, suggesting that the amount of GO is too little to alter the morphology of glucose HTC product (Figure 4f). However, the average diameter of the spheres had increased to micrometers, and they were mostly interconnected, possibly due to the increased glucose concentration in the reaction vessel.

Control experiments have been performed studying the glucose HTC products in the presence of other graphitic seeds such as graphite, carbon nanotubes, high surface area activated carbon, hydrazine-reduced r-GO, and hydrothermally reduced r-GO. Figure 5a,c,e,g displays SEM images showing the morphology of multiwalled carbon nanotubes, activated carbon, hydrazine-reduced GO, and HTC-treated GO, respectively. They were added into the glucose solution at a seed/glucose weight ratio of 1:50. Even at such high seed concentration, the main HTC product was carbon spheres, and no significant morphological change was observed for graphite (not shown here), carbon nanotubes (Figure 5b), and activated carbon (Figure 5d). The hydrazine-reduced r-GO (Figure 5f) and HTC-reduced r-GO (Figure 5h) appeared to grow a bit thicker. For graphite, carbon nanotubes, and carbon black, their inability to catalyze HTC reactions could be attributed to their lack of hydrophilic surface functional groups to seed the growth of glucose-derived carbon. The chemically and hydrothermally reduced r-GO samples

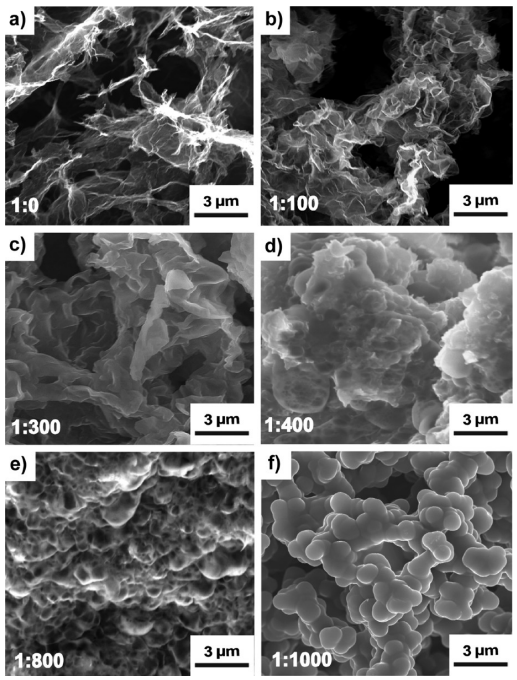

Figure 4. (a–e) SEM images of the HTC products of GO and glucose obtained with increase glucose content (1:0, 1:100, 1:300, 1:400, and 1:800) show that GO suppresses the formation of carbon spheres with GO/glucose ratio up to 1:800. (f) When even higher content of glucose (GO/glucose = 1:1000), the main product is carbon spheres, similar to those shown in Figure 1a.

should have many defects and residual oxygenated functional groups to promote carbon overgrowth. They are not as effective as GO, likely due to poorer water processability and less abundant functional groups. However, the graphitic surface also seems to be necessary for promoting HTC reactions. Additional control reactions showed that exfoliated phyllosilicate clay sheets, which are hydrophilic and do not have any aromatic functional domains on their basal plane, have nearly no effect on the HTC reaction of glucose. These results suggest that GO is unique or most effective in altering the morphology of HTC carbon. During glucose carbonization, the highly water-soluble glucose is gradually converted to more aromatic and hydrophobic materials.[14] Among the graphitic seed materials tested, GO is uniquely amphiphilic and exhibits similar hydrophilic–hydrophobic transition during hydrothermal reaction. Therefore, it can favorably interact with glucose, its reaction intermediates, as well as the final carbon product throughout the HTC reaction, thus making it most effective to seed the glucose carbonization product and template its growth. Kinetic study shown in Figure 3c also suggests that GO indeed promotes the nucleation of HTC carbon. Elemental analysis revealed that the C/O ratios of carbon spheres and hydrothermally treated GO are 1.8 and 4.5, respectively. GO-assisted HTC products were found to have higher C/O ratios. For example, the monoliths obtained from GO/glucose with a weight ratio of 1:100 and 1:400

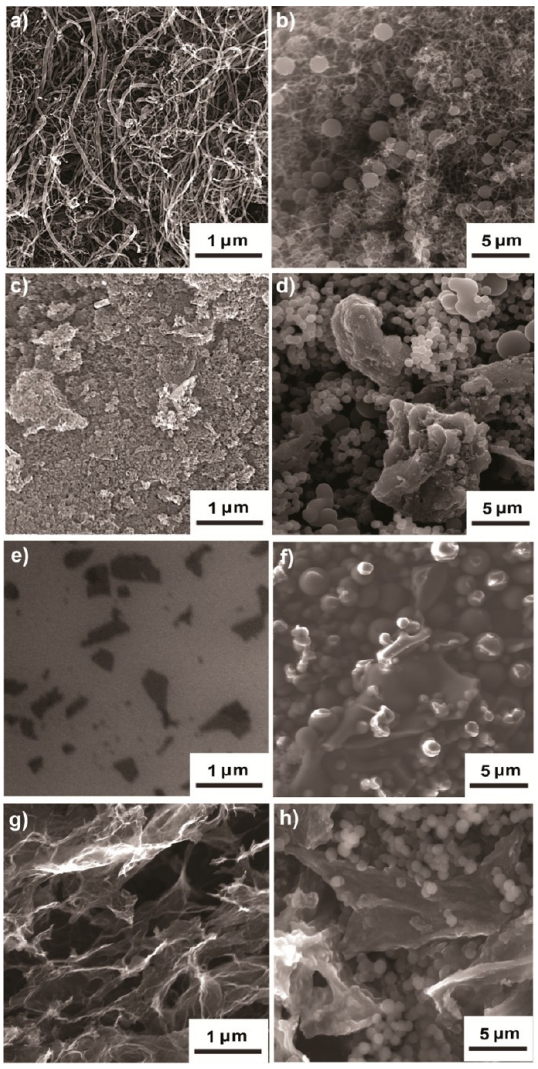

Figure 5. SEM images of alternative carbon materials tested for seeding HTC of glucose and the corresponding products. The SEM images in the left column are for (a) multiwalled CNTs, (c) activated carbon, (e) hydrazine-reduced r-GO, and (g) HTC-reduced r-GO. The images on the right are the corresponding HTC products. None of these carbon materials can suppress carbon sphere formation despite of the high seed concentration (2 wt %, seed to glucose ratio 1:50).

have C/O ratios of 2.7 and 2.2, respectively. Since the weight percentages of r-GO in the final products are relatively insignificant, the increased C/O ratios should be attributed to higher degree of carbonization, which is consistent with the results from FTIR and TGA studies shown in Figure 2.

The conductivities of the monolith samples were measured after pressing them under high pressure into pellets of known dimensions and weight. Silver electrodes were deposited on both ends of the pellets. Current was measured by sweeping the voltage between ±0.5 V. Specific conductivity normalized by density of the samples is plotted against the weight ratio of glucose to GO in the precursor (Figure 6c, open boxes). Pellets of carbon spheres and the HTC product from GO/glucose with a weight ratio of 1:1000 did not

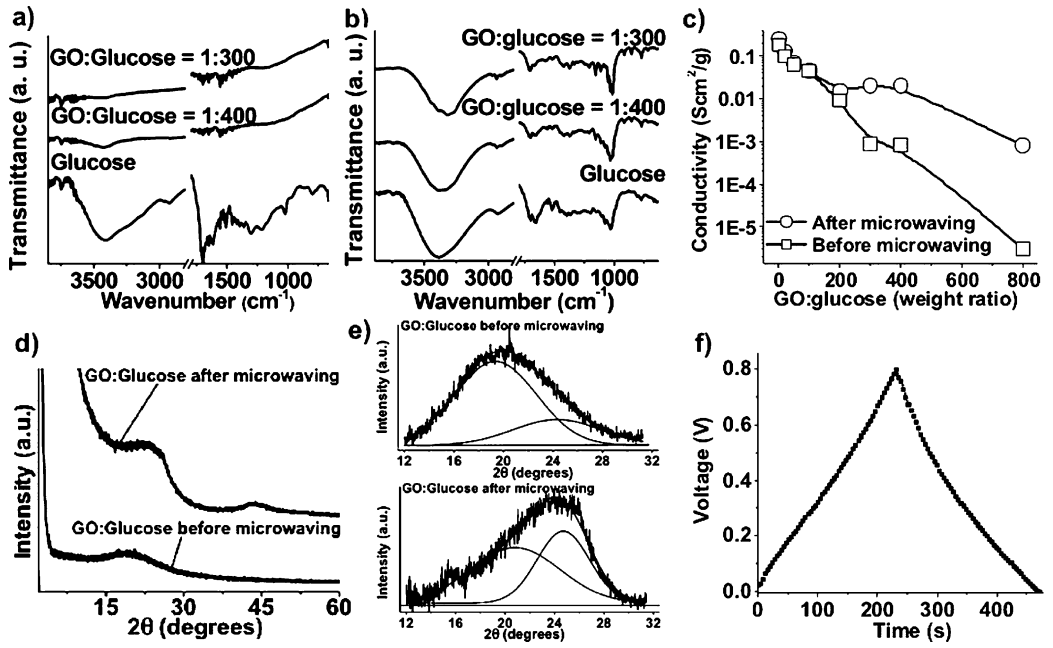

Figure 6. FTIR spectra of carbon spheres and monoliths obtained from HTC products made of different ratios of GO and glucose (a) before and (b) after microwave treatment for 1 min. (c) Conductivity of the HTC products before and after microwave treatment on a semilog plot, as a function of glucose content in the starting reaction mixtures. The conductivity values are normalized by the density of the pellets measured. Conductivity enhancement is observed for all the samples after microwave treatment, which is more prominent for those started with higher glucose content. Note that, without adding GO, the HTC carbon spheres are insulating. (d) XRD patterns of GO/glucose HTC product (weight ratio = 1:400) before and after microwave treatment. Increased degree of graphitization is observed after microwave treatment as indicated by the emergence of a graphite (100) peak at around 45° and (e) increased relative intensity of a graphite (002) band near 26°. (f) Galvanostatic charge/discharge curve of a supercapacitor prepared from microwave-treated GO/glucose monolith with 1:400 weight ratio.

show any current above the detection limit of the instrument (1 nA). However, all the other samples with GO/glucose ratio up to 1:800 were found to be conductive. The 1:300 and 1:400 samples exhibit electrical conductivity of around 0.8 $mScm^2\ g^{-1}$, which increased with increasing GO concentrations in the precursor solutions and reached 95 $mScm^2\ g^{-1}$ for sample prepared with 1:20 GO/glucose weight ratio. Pure r-GO monolith exhibited a conductivity of 200 $mScm^2\ g^{-1}$. The sample prepared with 1:800 GO glucose ratio also showed a small conductivity value of 3 $\mu Scm^2\ g^{-1}$. It is remarkable that a tiny fraction of GO in the starting reaction mixture has induced conductivity in large amounts of a material, which is otherwise an insulator. Although the embedded r-GO sheets also act as conducting channels, to generate measurable conductivity at a macroscopic level, the thick layer of glucose-derived carbon should be able to support electron transport. In fact, casted thin films made of the platelets shown in Figure 1b were also found to be conductive. Since in such thin films the r-GO sheets embedded in the platelets are largely parallel aligned and not in direct contact with each other, it suggests that the glucose-derived carbon coating the r-GO sheets must be conductive, as well.

While the use of GO seeds already improves the carbonization of glucose and leads to products with higher degree of carbonization and conductivity, one can take advantage of the embedded r-GO sheets to further improve degree of carbonization through microwave treatment. We found that 5 min of microwave treatment of carbon spheres using a 1250 W commercial microwave oven did not make them conductive. In contrast, microwaving of GO-seeded HTC products for just 1 min significantly improved their conductivity (Figure 6c, open circles). For example, the normalized conductivity of the sample prepared with GO/glucose ratio of 1:400 increased from 0.8 to 20 $mScm^2\ g^{-1}$ after 1 min of microwave irradiation. r-GO sheets are strongly microwave absorbing[40,41] and thus can act as an *in situ* heating element for rapidly annealing the surrounding HTC carbon materials. The IR spectra of the samples before and after microwave irradiation are shown in Figure 6a,b, respectively. Indeed, drastic reduction in the −OH band intensity around 3400 cm^{-1} is observed for the GO-seeded HTC samples, except for the carbon spheres obtained from neat glucose. Elemental analysis also confirmed significant increase in degree of carbonization after microwave treatment. For example, the C/O ratio of HTC-treated GO/glucose monoliths of weight ratio 1:400 increased from 2.2 to 12.5 after 1 min microwave treatment, while that of the carbon spheres did not change after being microwaved for 5 min. X-ray diffraction (XRD) patterns

(Figure 6d) of GO/glucose HTC product (1:400 weight ratio) before and after microwave treatment show that microwave heating has increased the degree of graphitization. After microwave treatment, a new peak centered at around 45° emerged, which corresponds to graphite (100) diffraction. Moreover, the broad peak at lower angle shifted from near 20 to 24°. Deconvolution of this peak reveals the relative intensity, as indicated by the increase in the intensity of the diffraction band center.

Making biomass-derived carbon materials conductive using catalytic amounts of GO and further through r-GO-assisted rapid microwave heating can lead to their more useful applications in electronics without significantly increasing material or processing cost. As a proof of concept, we have examined the performance of a microwave-treated monolith obtained from the GO/glucose precursor with a weight ratio of 1:400 as ultracapacitor electrodes. Two-electrode symmetric coin cells were assembled with 5 M KOH of aqueous solution as the electrolyte. Figure 6e shows a typical cycle of charge/discharge curves of the resulting ultracapacitor device with a constant current density of 1 A/g. Symmetric and nearly linear charge/discharge curve was obtained, indicating excellent reversibility and high Coulombic efficiency. The specific capacitance value was calculated to be 140 F/g based on the weight of the active material on the electrode. The weight percentage of r-GO present in the final microwave can be calculated by the following. In a control experiment, 15 mg of GO was converted to a monolith of 4 mg after HTC and microwave treatments under the same conditions. The final weight of the monolith prepared from 15 mg of GO and 6 g of glucose was found to be around 390 mg after microwaving. If we assume that GO inside the monolith undergoes the same extent of mass loss as neat GO after HTC and microwave treatments, the final product would contain around 1% of r-GO. Note that the specific capacitance of neat r-GO monolith prepared by HTC treatment has been reported to be around 160 F/g.[39] Therefore, the specific capacitance of 140 F/g should be largely contributed by the glucose-derived carbon. It is also quite remarkable that adding such a small amount of GO in the starting reaction mixture and 1 min of microwave treatment has transformed an otherwise insulating material into conductive carbon materials with specific capacitance value as good as many reported values for graphene itself.[39,42] Further, the Coulombic efficiency was close to 100% in the whole 1000 cycles (Figure 6f).

Parallel experiments done with cellulose revealed that GO has a similar effect in enhancing its HTC product. The starting white cellulose powders are made of irregularly shaped particles with sizes in the range of tens to hundreds of micrometers (Figure 7a,b). After HTC at 230 °C for 16 h, dark brown powders of carbon spheres with a diameter around 1−4 μm were recovered from the resulting dispersion (Figure 7c,d). Adding 1 wt % of GO to cellulose changed the HTC product from a carbon sphere dispersion to a free-standing monolith. SEM examination of the freeze-dried sample showed the presence of thick wrinkled platelets (Figure 7f) similar to those observed in GO/glucose HTC products. Elemental analysis shows that these samples have a C/O ratio of 4, while cellulose-derived carbon spheres gave a C/O ratio of 3. The higher degree of carbonization is also evident by the black color of the GO/cellulose HTC product. The threshold GO/cellulose weight ratio that can suppress carbon sphere formation is found to be around 1:300.

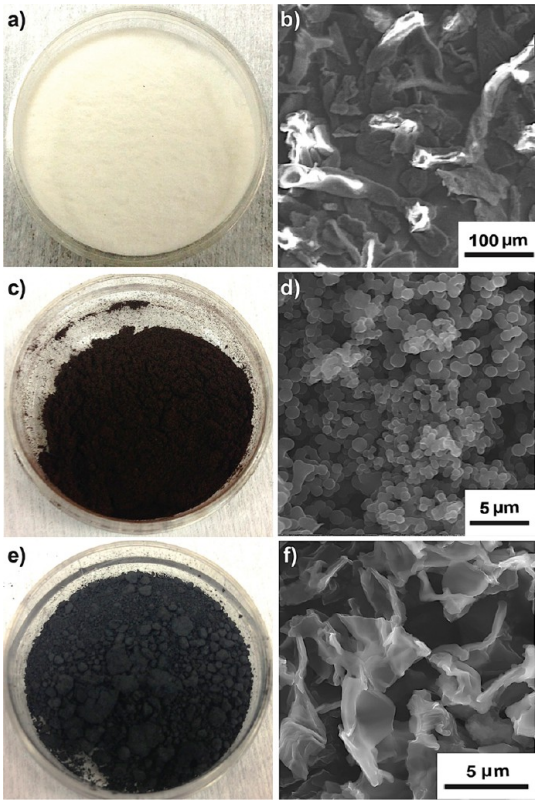

Figure 7. GO-assisted HTC of cellulose. Photos of (a) pure cellulose, (c) its HTC product, and (e) product obtained from GO/cellulose mixture (weight ratio 1:100) after HTC treatment at 230 °C for 16 h. (b,d,f) SEM images corresponding to (a), (c), and (e), respectively. HTC treatment converts (b) sub-millimeter-sized cellulose particles into (d) few-micrometer-sized carbon spheres. However, in the presence of GO, the HTC product shows thick sheet-like morphology.

CONCLUSION

The work here demonstrates that adding a small amount of GO can greatly improve the properties of biomass-derived carbon without significantly increasing the cost of materials or materials processing. HTC of glucose and cellulose typically produces insulating micrometer-sized carbon spheres. However, HTC of GO and glucose resulted in thick platelets of glucose-derived carbon-coated r-GO sheets at low GO

concentration. At high GO concentration, electrically conductive r-GO-supported carbon monoliths were obtained. Adding 0.12 wt % of GO to glucose can already significantly alter the morphology and improve the degree of carbonization and conductivity of its HTC carbon product. Moreover, adding GO can significantly accelerate the carbonization reaction. While glucose-derived carbon spheres cannot be effectively heated by microwave, the embedded r-GO sheets in the HTC product can serve as an *in situ* microwave heating element for rapidly annealing the resulting carbon composite to further increase the degree of carbonization, graphitization, and conductivity. One minute of microwave processing in a commercial oven was able to enhance the conductivities of the HTC products by many orders of magnitude, making them readily useful for applications such as electrodes for ultracapacitors.

MATERIALS AND METHODS

GO was prepared by a modified Hummers' method[43] and purified by two-step washing of HCl and acetone as reported earlier.[44] A 15 mL aqueous dispersion of GO was mixed with different amounts of glucose and annealed inside a Teflon-lined autoclave at 180 °C for 16 h. The concentration of GO was varied from 0.02 to 1 mg/mL. The weight ratio of GO and glucose was adjusted from 1:0 to over 1:800. HTC of cellulose was performed at a higher temperature of 230 °C. The HTC monoliths were freeze-dried for 6 h before characterization. Microwave treatment was done by irradiating the freeze-dried monoliths in a commercial microwave oven of 1250 W for 1 min. For conductivity measurements, samples were densified under high pressure (41 MPa) and then cut into rectangular pellets of known dimensions and weight. Silver electrodes were deposited on either end of the pellet. A Keithley 2601A source meter was used to measure the currents between two electrodes by sweeping the voltage between ±0.5 V. For electrochemical characterization, microwave-treated 1:400 GO/glucose monoliths were grinded and mixed with polytetrafluoroethylene (PTFE) solution (5% in isopropyl alcohol) in a weight ratio of 1:60 (PTFE/monolith) and then drop-casted on stainless steel current collectors (~3 mg of sample per electrode was maintained). The capacitor electrodes made as such were characterized by constant current charge/discharge with two symmetric electrodes in a CR2016-type coin cell using an Autolab electrochemical interface instrument (PGSTAT 302N). Waterman, grade no. 4 filter paper was used as the separator with 5 M KOH solution as the electrolyte.

Conflict of Interest: The authors declare no competing financial interest.

Acknowledgment. D.K. acknowledges the support from the Ryan Fellowship and the Northwestern University International Institute for Nanotechnology. K.R. acknowledges the Indo-US Science & Technology Forum (IUSSTF) for a postdoctoral fellowship. J.S. acknowledges the China Scholarship Council for an exchange student fellowship. J.H. acknowledges the Alfred P. Sloan Foundation for a Sloan Research Fellowship, the Sony Corporation for a gift donation, and the NSF for a CAREER Award (DMR 0955612). The authors are also grateful for the use of experimental facilities at the Northwestern University Atomic- and Nanoscale Characterization Experimental Center (NUANCE, EPIC, NIFTI, Keck-II), and the J.B. Cohen X-Ray Diffraction Facility supported by the MRSEC program of the National Science Foundation (DMR-1121262) at the Materials Research Center of Northwestern University.

REFERENCES AND NOTES

1. Hu, B.; Wang, K.; Wu, L. H.; Yu, S. H.; Antonietti, M.; Titirici, M. M. Engineering Carbon Materials from the Hydrothermal Carbonization Process of Biomass. *Adv. Mater.* **2010**, *22*, 813–828.
2. Cakan, R. D.; Titirici, M. M.; Antonietti, M.; Cui, G. L.; Maier, J.; Hu, Y. S. Hydrothermal Carbon Spheres Containing Silicon Nanoparticles: Synthesis and Lithium Storage Performance. *Chem. Commun.* **2008**, 3759–3761.
3. Paraknowitsch, J. P.; Thomas, A.; Antonietti, M. Carbon Colloids Prepared by Hydrothermal Carbonization as Efficient Fuel for Indirect Carbon Fuel Cells. *Chem. Mater.* **2009**, *21*, 1170–1172.
4. Titirici, M. M.; Antonietti, M.; Baccile, N. Hydrothermal Carbon from Biomass: A Comparison of the Local Structure from Poly- to Monosaccharides and Pentoses/Hexoses. *Green Chem.* **2008**, *10*, 1204–1212.
5. Titirici, M. M.; Antonietti, M.; Thomas, A. A Generalized Synthesis of Metal Oxide Hollow Spheres Using a Hydrothermal Approach. *Chem. Mater.* **2006**, *18*, 3808–3812.
6. Titirici, M. M.; Thomas, A.; Antonietti, M. Back in the Black: Hydrothermal Carbonization of Plant Material as an Efficient Chemical Process To Treat the Co_2 Problem? *New J. Chem.* **2007**, *31*, 787–789.
7. Titirici, M. M.; Thomas, A.; Yu, S. H.; Muller, J. O.; Antonietti, M. A Direct Synthesis of Mesoporous Carbons with Bicontinuous Pore Morphology from Crude Plant Material by Hydrothermal Carbonization. *Chem. Mater.* **2007**, *19*, 4205–4212.
8. Yu, S. H.; Cui, X. J.; Li, L. L.; Li, K.; Yu, B.; Antonietti, M.; Colfen, H. From Starch to Metal/Carbon Hybrid Nanostructures: Hydrothermal Metal-Catalyzed Carbonization. *Adv. Mater.* **2004**, *16*, 1636–1640.
9. Zhang, P. F.; Yuan, J. Y.; Fellinger, T. P.; Antonietti, M.; Li, H. R.; Wang, Y. Improving Hydrothermal Carbonization by Using Poly(ionic liquid)s. *Angew. Chem., Int. Ed.* **2013**, *52*, 6028–6032.
10. Liang, H. W.; Guan, Q. F.; Chen, L. F.; Zhu, Z.; Zhang, W. J.; Yu, S. H. Macroscopic-Scale Template Synthesis of Robust Carbonaceous Nanofiber Hydrogels and Aerogels and Their Applications. *Angew. Chem., Int. Ed.* **2012**, *51*, 5101–5105.
11. Bergius, F. Formation of Anthracite. *Z. Elektrochem.* **1913**, *19*, 858–860.
12. Berl, E.; Schmidt, A. On the Emergence of Carbon. II. The Incarbonic Nature of Cellulose and Lignin in a Neutral Medium. *Justus Liebigs Ann. Chem.* **1932**, *493*, 97–123.
13. Berl, E.; Schmidt, A.; Koch, H. The Development of Carbon. *Angew. Chem.* **1932**, *45*, 0517–0519.
14. Sun, X. M.; Li, Y. D. Colloidal Carbon Spheres and Their Core/Shell Structures with Noble-Metal Nanoparticles. *Angew. Chem., Int. Ed.* **2004**, *43*, 597–601.
15. Wang, Q.; Li, H.; Chen, L. Q.; Huang, X. J. Novel Spherical Microporous Carbon as Anode Material for Li-Ion Batteries. *Solid State Ionics* **2002**, *152*, 43–50.
16. Titirici, M. M.; White, R. J.; Falco, C.; Sevilla, M. Black Perspectives for a Green Future: Hydrothermal Carbons for Environment Protection and Energy Storage. *Energy Environ. Sci.* **2012**, *5*, 6796–6822.
17. Titirici, M. M.; Antonietti, M. Chemistry and Materials Options of Sustainable Carbon Materials Made by Hydrothermal Carbonization. *Chem. Soc. Rev.* **2010**, *39*, 103–116.
18. Bai, H.; Li, C.; Shi, G. Q. Functional Composite Materials Based on Chemically Converted Graphene. *Adv. Mater.* **2011**, *23*, 1089–1115.
19. Luo, J.; Kim, J.; Huang, J. Material Processing of Chemically Modified Graphene: Some Challenges and Solutions. *Acc. Chem. Res.* **2013**, *46*, 2225–2234.
20. Park, S.; Ruoff, R. S. Chemical Methods for the Production of Graphenes. *Nat. Nanotechnol.* **2009**, *4*, 217–224.
21. Li, D.; Kaner, R. B. Materials Science: Graphene-Based Materials. *Science* **2008**, *320*, 1170–1171.

22. Eda, G.; Chhowalla, M. Chemically Derived Graphene Oxide: Towards Large-Area Thin-Film Electronics and Optoelectronics. *Adv. Mater.* **2010**, *22*, 2392–2415.
23. Compton, O. C.; Nguyen, S. T. Graphene Oxide, Highly Reduced Graphene Oxide, and Graphene: Versatile Building Blocks for Carbon-Based Materials. *Small* **2010**, *6*, 711–723.
24. Huang, X.; Qi, X. Y.; Boey, F.; Zhang, H. Graphene-Based Composites. *Chem. Soc. Rev.* **2012**, *41*, 666–686.
25. Kim, J.; Cote, L. J.; Huang, J. X. Two Dimensional Soft Material: New Faces of Graphene Oxide. *Acc. Chem. Res.* **2012**, *45*, 1356–1364.
26. Kim, J. E.; Han, T. H.; Lee, S. H.; Kim, J. Y.; Ahn, C. W.; Yun, J. M.; Kim, S. O. Graphene Oxide Liquid Crystals. *Angew. Chem., Int. Ed.* **2011**, *50*, 3043–3047.
27. Dreyer, D. R.; Park, S.; Bielawski, C. W.; Ruoff, R. S. The Chemistry of Graphene Oxide. *Chem. Soc. Rev.* **2010**, *39*, 228–240.
28. Krishnan, D.; Kim, F.; Luo, J. Y.; Cruz-Silva, R.; Cote, L. J.; Jang, H. D.; Huang, J. X. Energetic Graphene Oxide: Challenges and Opportunities. *Nano Today* **2012**, *7*, 137–152.
29. Loh, K. P.; Bao, Q. L.; Eda, G.; Chhowalla, M. Graphene Oxide as a Chemically Tunable Platform for Optical Applications. *Nat. Chem.* **2010**, *2*, 1015–1024.
30. Erickson, K.; Erni, R.; Lee, Z.; Alem, N.; Gannett, W.; Zettl, A. Determination of the Local Chemical Structure of Graphene Oxide and Reduced Graphene Oxide. *Adv. Mater.* **2010**, *22*, 4467–4472.
31. Kim, J.; Cote, L. J.; Kim, F.; Yuan, W.; Shull, K. R.; Huang, J. X. Graphene Oxide Sheets at Interfaces. *J. Am. Chem. Soc.* **2010**, *132*, 8180–8186.
32. Cote, L. J.; Kim, J.; Tung, V. C.; Luo, J. Y.; Kim, F.; Huang, J. X. Graphene Oxide as Surfactant Sheets. *Pure Appl. Chem.* **2011**, *83*, 95–110.
33. Xu, Y. X.; Zhao, L.; Bai, H.; Hong, W. J.; Li, C.; Shi, G. Q. Chemically Converted Graphene Induced Molecular Flattening of 5,10,15,20-Tetrakis(1-methyl-4-pyridinio)-porphyrin and Its Application for Optical Detection of Cadmium(II) Ions. *J. Am. Chem. Soc.* **2009**, *131*, 13490–13497.
34. Bao, Y.; Song, J. X.; Mao, Y.; Han, D. X.; Yang, F.; Niu, L.; Ivaska, A. Graphene Oxide-Templated Polyaniline Microsheets toward Simultaneous Electrochemical Determination of AA/DA/UA. *Electroanalysis* **2011**, *23*, 878–884.
35. Luo, J. Y.; Tung, V. C.; Koltonow, A. R.; Jang, H. D.; Huang, J. X. Graphene Oxide Based Conductive Glue as a Binder for Ultracapacitor Electrodes. *J. Mater. Chem.* **2012**, *22*, 12993–12996.
36. Tung, V. C.; Kim, J.; Cote, L. J.; Huang, J. X. Sticky Interconnect for Solution-Processed Tandem Solar Cells. *J. Am. Chem. Soc.* **2011**, *133*, 9262–9265.
37. Sakaki, T.; Shibata, M.; Miki, T.; Hirosue, H.; Hayashi, N. Reaction Model of Cellulose Decomposition in Near-Critical Water and Fermentation of Products. *Bioresour. Technol.* **1996**, *58*, 197–202.
38. Zhou, Y.; Bao, Q. L.; Tang, L. A. L.; Zhong, Y. L.; Loh, K. P. Hydrothermal Dehydration for the "Green" Reduction of Exfoliated Graphene Oxide to Graphene and Demonstration of Tunable Optical Limiting Properties. *Chem. Mater.* **2009**, *21*, 2950–2956.
39. Xu, Y. X.; Sheng, K. X.; Li, C.; Shi, G. Q. Self-Assembled Graphene Hydrogel *via* a One-Step Hydrothermal Process. *ACS Nano* **2010**, *4*, 4324–4330.
40. Zhu, Y. W.; Murali, S.; Stoller, M. D.; Velamakanni, A.; Piner, R. D.; Ruoff, R. S. Microwave Assisted Exfoliation and Reduction of Graphite Oxide for Ultracapacitors. *Carbon* **2010**, *48*, 2118–2122.
41. Singh, V. K.; Shukla, A.; Patra, M. K.; Saini, L.; Jani, R. K.; Vadera, S. R.; Kumar, N. Microwave Absorbing Properties of a Thermally Reduced Graphene Oxide/Nitrile Butadiene Rubber Composite. *Carbon* **2012**, *50*, 2202–2208.
42. Stoller, M. D.; Park, S. J.; Zhu, Y. W.; An, J. H.; Ruoff, R. S. Graphene-Based Ultracapacitors. *Nano Lett.* **2008**, *8*, 3498–3502.
43. Hummers, W. S.; Offeman, R. E. Preparation of Graphitic Oxide. *J. Am. Chem. Soc.* **1958**, *80*, 1339–1339.
44. Kim, F.; Luo, J. Y.; Cruz-Silva, R.; Cote, L. J.; Sohn, K.; Huang, J. X. Self-Propagating Domino-like Reactions in Oxidized Graphite. *Adv. Funct. Mater.* **2010**, *20*, 2867–2873.